UCRL- 85957
PREPRINT
CONF-811040--12

DESIGN OF 12-T YIN-YANG MAGNETS OPERATING IN SUBCOOLED, SUPERFLUID HELIUM

D. N. CORNISH and R. W. HOARD,
R. BALDI. (GENERAL DYNAMICS)

This paper was prepared for submittal to
Ninth Symposium on Engineering Problems of Fusion Research
Chicago, Illinois. October 26-29, 1981

October 9, 1981

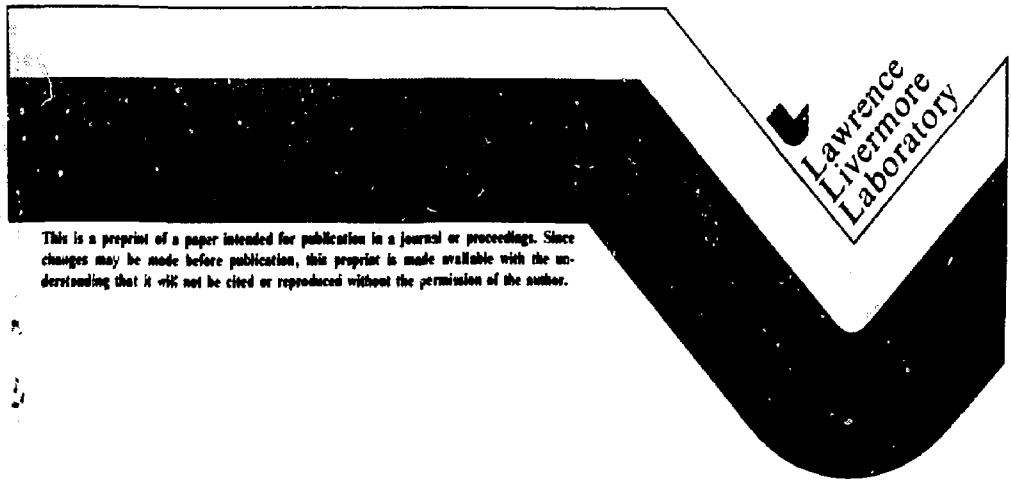

DESIGN OF 12-T YIN-YANG MAGNETS OPERATING IN SUBCOOLED, SUPERFLUID HELIUM*

D. N. Cornish and R. W. Hoard
Lawrence Livermore National Laboratory, University of California
Livermore, CA

R. Baldi
General Dynamics, Convair Division
San Diego, CA

Summary

A conceptual design study of a large 12-T yin-yang pair of coils, typical of the plug coils envisioned for a tandem-mirror facility to follow MFTF, has been completed. Because of its larger size and field strength, the magnetic forces are much greater than those experienced on MFTF. The main purpose of this study, therefore, is to assess the feasibility of such a device, paying particular attention to mechanical stress and conductor strain.

The conductor proposed operates at 15.6 kA and consists of a rectangular half-hard copper stabilizer with a Nb-Ti insert in the low-field regions and Nb_3Sn in the high field. The coil is divided into four sections in the longitudinal direction, with steel substructure to limit the winding stress to an acceptable level. The conductor is cryostatically stabilized in superfluid He at 1.8 K and 1.2 atm, with an operating heat flux of 0.8 $W \cdot cm^{-2}$.

We conclude that the building of such a magnet system should be possible with modest extensions to present-day technologies.

Introduction

During 1980, a preliminary design study of a Tandem Mirror Next Step (TMNS) facility to follow the Mirror Fusion Test Facility (MFTF) was carried out.[1] The facility was designed to demonstrate the engineering feasibility of a tandem mirror reactor and was based on a deuterium-tritium burning device having a fusion power output of 245 MW. The magnetic configuration is shown in a computer drawing reproduced in Fig. 1, and the design field strengths and dimensions are given in Table I. Design constraints were that the maximum field on the conductor, assumed to be Nb_3Sn, would be 12 T and that the overall current density in the winding area would be limited to 2×10^7 $A \cdot m^{-2}$.

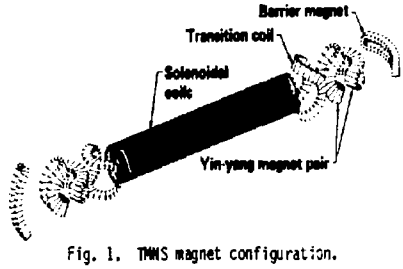

Fig. 1. TMNS magnet configuration.

The 12-T yin-yang magnet pair represents a considerable advance in superconducting magnet technology from that required for MFTF. A study has therefore been carried out in conjunction with the Convair Division of General Dynamics to assess the feasibility of building such a magnet system and to check the assumptions made. This paper summarizes the results of this design study.

Table I.
Design Field Strength and Dimensions for TMNS Magnet.

Central-cell uniform field (T	2.5
Yin-yang-cell mirror (T)	9.0
Yin-yang-cell minimum (T)	6.0
Barrier well (T)	1.8
Barrier mirror (T)	9.0
Yin-yang-cell plasma radius (m)	0.56
Central-cell plasma radius (m)	0.83
Central-cell length (effective) (m)	50.90

12-T Yin-Yang Design Parameters

The initial design requirement parameters of the yin-yang coil are summarized in Table II.

Table II. Initial Design Parameters for 12-T Yin Yang.

Major radius (m)	3.7
Minor radius (m)	1.5
Sweep angle (degree)	65
Coil section (m)	2.72 x 0.68
Current density ($A \cdot m^{-2}$)	2.04×10^7
Amp-turns per coil (AT)	3.77×10^7
Total magnetic energy (J)	10^{10}
Maximum field at conductor (T)	12

It was found on MFTF that the cumulative, transverse crushing pressure exerted by the magnetic field on the conductor was approaching the safe limit. It was thus clear that this stress would be of major concern on TMNS, where the dimensions, field, and total amp-turns are very much higher. Figure 2 shows how the longitudinal pressure builds up across sections taken at the center of the major and minor radii; lateral stresses are about two-thirds of these values. The total stress on the conductor is increased still further by tension in the conductor, which is discussed in detail later in the paper. If the conductor is assumed to be cryostatically stabilized in pool-boiling helium, the local stress exerted by the interturn and interlayer insulation will be approximately double this. Additional steps must be taken if these very large forces are to be safely accommodated and a reasonable overall current density maintained.

The first assumption made was that the conductor should be operated in subcooled superfluid helium, operating at 1.8 K and 1.2 atm. The improved heat-

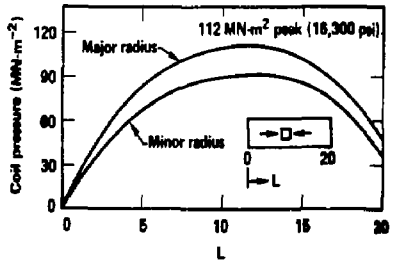

Fig. 2. Coil pack longitudinal magnetic pressure.

*Work performed under the auspices of the U.S. Department of Energy by the Lawrence Livermore National Laboratory under contract number W-7405-ENG-48.

transfer characteristics obtained under these conditions would help to compensate for the increased stabilizer resistivity resulting from magneto-resistance at 12 T and the cold-working carried out to increase its yield stress. Next, a number of different methods of introducing structure into the winding area to limit the cumulative stress to an acceptable value were studied.

The arrangement finally adopted was to split each coil into a number of nested coils, as shown in Figs. 3 and 4. Each section is separately wound on its own L-shaped coil form, to which is welded the other L-section, after winding, so that each coil is sealed in its own case. Each section is then fitted with a stainless-steel bladder, ultimately to be injection-filled with urethane, a technique developed for MFTF. Final assembly of the coils on the structural case is carried out in sequence. Section (1) is assembled first, followed by welding the first substructure to the backplate and so on, until all four sections have been assembled and welded into the structural case.

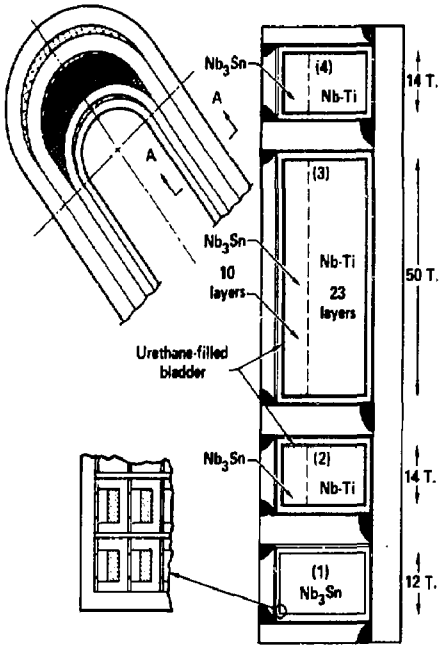

Fig. 3. Arrangement of yin-yang coils and structural case.

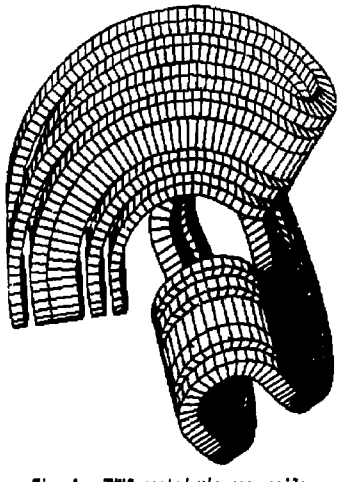

Fig. 4. TMNS nested yin-yang coils.

The maximum field at the conductor of the original design was somewhat higher than the assumed value of 12 T. The increased amp-turns required to give the necessary field in the plasma, allowing for the space occupied by the substructure, increases this still further to approximately 14 T at the inside of the minor radius. The limiting value of 12 T is obtained by inserting space between the turns at the minor radius only, as shown in Fig. 3. The revised coil parameters are listed in Table III.

Table III. Revised Coil Parameters.

Stored energy per yin yang (J)	1.33×10^{10}
Amp-turns per coil (AT)	4.633×10^{7}
Turns per coil	2970
Winding area including substructure (m)	3.75 x 0.70
Average current density ($A \cdot m^{-2}$)	1.76×10^{7}

Conductor Design

Different conductor configurations were studied, and the one finally chosen is shown in Fig. 5, its details being summarized in Table IV.

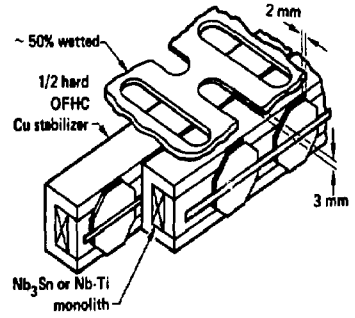

Fig. 5. TMNS conductor and inter-turn insulation.

Table IV. Conductor Data.

Superconductor	Nb-Ti	Nb_3Sn
Operating current (A)	15,600	15,600
I_c at 1.8 K, 12 T (A)	---	22,286
I_c at 1.8 K, 9 T (A)	22,286	---
Winding current density ($MA \cdot m^{-2}$)	23.67	23.67
Ratio, Cu:non-Cu	13:1	10:1
Conductor length (km)	111	61
Heat flux ($W \cdot cm^{-2}$)	0.8	0.8
Stabilizer resistance ratio	75:1	75:1
Core dimensions (cm)	0.594 x 1.656	
Overall dimensions (cm)	1.932 x 2.791	

The Nb_3Sn superconductor is used in all regions where the field is greater than 9 T. This conductor is therefore used for the innermost section, Section 1, and for the first 10 of the 33 layers in each of the remaining sections.

Based on 2600-foot lengths of conductor being available, there are 163 conductor joints per coil. All these joints are made in the region of the small

radius, and the space added in this region to reduce the peak field is an ideal location for them. The proposed method for making the joint is to machine off the stabilizer on one of the wide faces for 12 inches at the end of each conductor and to overlap the exposed superconductor, inserting a thin indium foil between them. Thirty-six-in.-long copper cover plates are then tightly clamped around the joint, and the whole is then soldered together using Pb-Sn eutectic: the ends of the cover plates are tapered to blend the joint to the conductor dimensions. The resistance of the joint is estimated to be approximately 0.5×10^{-9} ohms.

Cryostatic Stability

This section summarizes the results of conductor stability calculations which are reported in detail in Ref. 2.

To ensure stability, a number of criteria must be met:

1. Kapitza Resistance. When a surface immersed in He II is heated, a temperature gradient is developed across a boundary layer, a few microns thick. For copper, this takes the form

$$q = 0.02 \left(T^4 - T_b^4\right) \text{ W·cm}^{-2}, \text{ where} \qquad (1)$$

q = Heat transfer from the surface (W·cm^{-2}),
T = Surface temperature (K),
T_b = Bath temperature (K).

For the proposed conductor, $q = 0.8$ W·cm^{-2}; therefore, $T = 2.65$ K, which is less than current-sharing temperatures which are 4.2 and 2.83 K for the Nb_3Sn and Nb-Ti conductors, respectively.

2. Critical Heat Flux Along Cooling Channels. There is an upper limit to the heat flux which can be transported by He II along a cooling channel. The value of this is given by the expression

$$\text{Critical heat flux} = q_c = \frac{\alpha}{L^{1/3}} \text{ W·cm}^{-2}, \qquad (2)$$

where α = constant = 7.4, L = channel length.

When considering a conductor in the midst of the winding, it is seen that there are eight channels feeding coolant to it: four vertical and four horizontal. When the conductor is fully normal, the heat generated is 3.38 W·cm^{-1}. We have taken the length of the channel to be one and one-half conductor pitches, which is the distance from the center line of one conductor to the furthest corner of the adjacent conductor: at this point the number of cooling channels doubles, which halves the heat flux.

It is shown in Ref. 2 that the error introduced by computing the critical heat flux from the parameters of the first one and one-half pitch channel length is only a few percent. Thus, using 4.586 and 3.198 cm and 0.222 and 0.577 cm^2 for the vertical and horizontal channel length and area, we get

q_h (max) = 3.97 W·cm^{-2} and q_v (max) = 3.52 W·cm^{-2}. The critical fluxes, using Eq. 2 are

q_h (max) = 5.02 W·cm^{-2}, and q_v (max) = 4.45 W·cm^{-2}. Hence the current at which the heat flux reaches the critical value is

$$\left(\frac{5.02 + 4.45}{3.97 + 3.52}\right)^{(1/2)} \times 15.6 = 17.5 \text{ kA}.$$

Extending the theory of Maddock et al.,[3] we get a "cold-end" recovery current of 19.85 kA.

3. Transient Stability. The above calculations assume that there is a sufficient reservoir of He II to supply the heat load for the whole time that the conductor is normal. In practice, the supply runs out when the total heat input equals the change in enthalpy of the He II (in effective contact with the conductor) between 1.8 and 2.17 K. Using the work of Claudet et al.[4] to estimate the value of the effective volume of He II, we calculate that it will take about 80 s for the He II system to revert to He I.

Stress Analysis

Stresses in the case and conductor have also been estimated.

1. Case Magnetic Loads. Case overall magnetic loads have been calculated, assuming the conductor to be fully flexible and non-load bearing (Fig. 6).

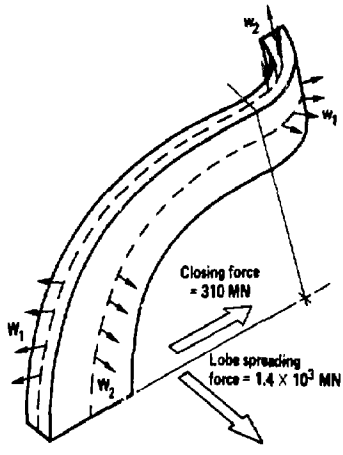

Load	Peak pressure (MN·m^{-2})	Average pressure (MN·m^{-2})	Line load (MN·m^{-1})
W_1	48.5	46.4	31.5
W_2	49.2	39.1	108.3
W_1	58.5	53.0	144.3
W_2	61.8	28.8	196.6

Fig. 6. TMNS yin-yang magnet case loads.

2. Stresses and Strains. The following radial deflections all contribute towards axial strain in the conductor:

a. Overall case deflection
b. Local case deflection
c. Take-up of winding gaps (assumed to be 0.002 in./layer)
d. Winding compaction as calculated using STAMSOL II computer code

Evaluations of the above at both the major and minor radii (Fig. 7) were added to the compressive stresses to give the total conductor stress. It was assumed that the strain in the stabilizer and superconductor were identical and that the half-hard stabilizer maintained a linear stress-strain curve, while that of the annealed superconductor was allowed to be nonlinear. The maximum Von Mises values are

$\sigma_{Cu} = 241$ MN·m^{-2} (35 ksi), $\sigma_{s/c} = 124$ MN·m^{-2} (18 ksi),

$\varepsilon = 0.214\%$.

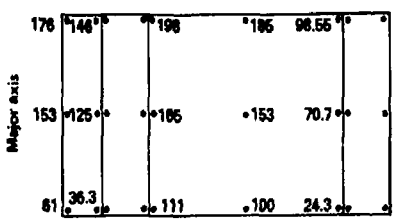

Fig. 7. Conductor tensile stresses (in $MN \cdot m^{-2}$) at major and minor radii.

Table V lists the various contributions to the absolute value of strain in the Nb_3Sn superconductor. The working value varies from -0.45% to +0.08%, which is well within acceptable limits.

Table V. Superconductor Strains for Four Quadrants of Superconductor Cross Section.

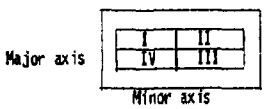

	Strain in quadrant			
	I (%)	II (%)	III (%)	IV (%)
Cooldown from reaction	-0.3	-0.3	-0.3	-0.3
Straightening	-0.09	-0.09	+0.09	+0.09
Winding[a]	-0.175	+0.175	+0.175	-0.175
Magnet cooldown	-0.1	-0.1	-0.1	-0.1
Magnetic forces	+0.214	+0.214	+0.214	+0.214
Total	-0.451	-0.101	+0.079	-0.271

[a]These are values for bending around the major radius, which is the worse case; values for the minor radius are +0.16, +0.16, -0.16, and -0.16, respectively.

When considering the stresses produced in the magnet case, it has been assumed that a third of the lobe-opening force is taken by the small radius of the case, and that the remainder of the opening force is taken by the external structure. The summation of all the case deflections results in a maximum case stress of 550 $MN \cdot m^{-2}$ (80 ksi), which is a safe working value for 304 LN stainless steel.

Coil Protection

The large amount of stored magnetic energy, coupled with the smaller quantity of stabilizer permitted by the use of He II as the coolant, increases the difficulty of protecting the coil in the event of a quench. It is therefore proposed that each coil be divided electrically into a number of sections, each with its own power supply and protection circuit. The power supplies will be computer controlled to keep them in synchronism, and the sections will be arranged to keep the maximum temperature and discharge voltages approximately the same. A full investigation of this aspect has not been carried out. However, if each coil is divided into five equal-energy sections, a discharge voltage of 1000 V per section would give a decay time constant of about 170 s and a maximum conductor temperature of less than 200 K.

Refrigeration Losses

Losses at 1.8 K require approximately three times the power consumption as those at 4.5 K, so we have studied the impact of this effect. It was assumed that, in addition to the normal LN shielding, there would be 4.5 K intercepts on the magnet supports and a 4.5 K shield outside the magnet structure. As can be seen from Table VI, the majority of the 1.8 K loss (any losses due to neutron heating have not been included) is generated in the conductor splices. This is probably the least accurate figure, and tests would need to be carried out on prototype splices to obtain a better value.

Table VI. Refrigeration Requirements.

Source	4.5 K (W)	1.8 K (W)
LN shield radiation	84.4	---
LN shield struts	133.9	---
LHe shield radiation	---	---
LHe shield struts	---	5.0
Supports	901.7	196.0
Coil splices	---	616.0
Instrument leads	242.7	2.0
Fluid leads	420.0	---
Total	1782.7	819.0
Current leads, five sets at 15.6 kA, 182 l/h		

Conclusions

We believe that this study has shown that the building of a 12-T yin-yang magnet of the size envisioned for TMNS is feasible with modest extensions to present-day technology. The proposed conductor is robust and relatively straightforward to fabricate. The very large forces can be accommodated by subdividing the winding. While this has increased the overall winding space, it has been done in a manner which should not seriously affect access to the plasma volume. The use of He II as the coolant has enabled higher values of conductor heat flux to be used and a good stability margin to be maintained.

Acknowledgments

We wish to acknowledge the detailed analysis work and conceptual proposals of the design team at General Dynamics. The services of Dr. S. Van Sciver, who educated us in the use and behavior of superfluid He, is also acknowledged. We would also like to thank Vergie Zuppan, the wizard of the Word Processor, for her help in compiling this paper.

References

1. C. C. Damm et al., Preliminary Design of a Tandem-Mirror-Next-Step Facility, Lawrence Livermore National Laboratory, UCRL-53060, (1980).

2. R. W. Hoard and D. N. Cornish, "Utilizing Superfluid He II in Multiple Interconnecting Magnet Coolant Channels," Lawrence Livermore National Laboratory, to be submitted to 8th International Cryogenic Engineering Conference, Kobe, Japan (1982).

3. B. J. Maddock, G. B. James, and W. T. Norris, "Superconductive Composites: Heat Transfer and Steady State Stabilization," in Cryogenics 9, p. 261 (1969).

4. G. Claudet and P. Seyfert, "Bath Cooling with Subcooled Superfluid Helium," Advances in Cryogenic Engineering (1981), Vol. 27, Paper KA-3 (to be published).